1. 遺伝子型タイピングチップを用いて

変異同定を試みた錐体桿体ジストロフィの1家系

吉田茂生[1)]、桑原留美[1)]、山地陽子[1)]、久保田敏昭[2)]、石橋達朗[1)]
([1)] 九州大、[2)]産業医大)

研究要旨 錐体桿体ジストロフィ(CORD)は錐体、桿体視細胞が障害される進行性の遺伝性疾患である。遺伝的異質性が高く、効率的な原因遺伝子同定法の確立が望まれる。今回、日本人 adCORD 患者に遺伝子型タイピングチップを用いた変異スクリーニングを試みた。対象は adCORD と診断した日本人発端者とその父親である。インフォームドコンセントを得た後に患者末梢血からゲノム DNA を抽出後、adCORD と原因遺伝子が部分的に合致するレーバー先天盲の変異部位を網羅した遺伝子型タイピングチップ(LCA チップ)による変異スクリーニングを行った。チップ解析で AIPL1、RPGRIP1、GUCY2D 遺伝子中に計 5 個の遺伝子多型を認め、この結果は全てダイレクトシークエンスと一致した。GUCY2D 遺伝子解析では、発端者および父親にチップ上にスポットされていない新規のミスセンス変異(2540A＞T、 2541G＞C、 2542A＞C)を認め、3 塩基変異とも同一のアリル上に存在した。日本人 adCORD 患者で GUCY2D 遺伝子の新規変異を同定した。適切な変異部位を網羅した遺伝子型タイピングチップを作成すれば、疾患原因遺伝子変異と疾患修飾遺伝子を同時にスクリーニングできる可能性が示唆された。

A. 研究目的

錐体ジストロフィ(Cone dystrophy ;COD) や錐体桿体ジストロフィ(cone-rod dystrophy ; CORD) は早期の錐体視細胞の変性による視力低下、色覚異常を特徴とする遺伝性網脈絡膜変性疾患の 1 つである。進行すると、錐体視細胞に続き桿体視細胞の変性がおこり、夜盲や周辺視野欠損などを生じる。 現在 CORD に対する効果的な治療はなく、その発症病因に基づいた治療の確立が望まれる。

CORD 遺伝子変異同定はその高い遺伝的異質性のため、まだ一般臨床で広く行われるには至っていない。従って様々な候補となる遺伝子から迅速、効率的な原因遺伝子の同定法の確立が望まれる。

近年のゲノム医科学の進歩により、遺伝子型タイピングチップの実用性が改善してきている。[1]様々な遺伝子型タイピングチップのうち、arrayed primer extention (APEX) 法は 5'末端でオリゴヌクレオチドを硝子基板の上に固定したものである。[2]このテクノロジーを用いてこれまで Stargardt 病や レーバー先天盲(LCA)などの遺伝子多型や変異のスクリーニングが行われてきている。[3] LCA チップはこれまでに明らかになっている 8 つの原因遺伝子(AIPL1、CRB1、CRX、GUCY2D、RPE65、RPGRIP1、MERTK、LRAT)

の遺伝子変化部位を網羅している。 LCA の原因遺伝子のうち AIPL1、CRX、GUCY2D は adCORD の原因でもあるため、LCA チップは、CORD の原因同定のための初期スクリーニングツールに用いうる可能性があると考えた。

B. 研究方法

ゲノム DNA の調整

遺伝子変異スクリーニングのためのゲノム DNA の抽出は以前同様標準化プロトコールを用いて行った。[4]

APEX 法を用いた解析

APEX 法を用いた解析プロトコールは www.asperbio.com; Asper Biotech,Ltd から入手可能である。 AIPL1、CRB1、CRX、GUCY2D、RPE65、RPGRIP1、MERTK、LRAT 遺伝子を polymerase chain reaction (PCR)法で増幅した。

GUCY2D 遺伝子解析

GUCY2D の 18 の全てのエキソンと AIPL 、RPGRIP1 の特定のエキソンを PCR 増幅し、Taq Dyedeoxy Terminator Cycle Sequencing Kit (Applied Biosystems、 Foster City、 CA)を用いて直接塩基配列決定を行った。

GUCY2D エキソン 10 と 13 の遺伝子多型を同定するため、日本人 68 名の健常コントロール(男性 35 名、女性 33 名)のゲノム DNA の直接塩基配列決定も行った。

GUCY2D アリルのサブクローニング

GUCY2D のエキソン 13 の PCR 断片を、添付マニュアルに基づいて TOPO-2 (Invitrogen、 San Diego、 California)を用いてサブクローニングした。[5] サブクローニングした断片は T7 primer を用いて塩基配列を決定した。

(倫理面への配慮)

本研究はヘルシンキ宣言 に則り、また九州大学病院倫理委員会の承認を得て行った。全ての患者からインフォームドコンセントを得た。

C. 研究結果

発端者は50歳の日本人男性である。両眼の10年以上前からの視力低下を主訴に九州大学病院眼科を紹介受診した。当科初診時矯正視力は両眼0.4であった。父親、父方の叔父と祖母に中心視野異常の家族歴があった。スリットによる診察では軽度の両眼白内障を認める以外に前眼部に異常を認めなかった。眼底検査では両眼に標的黄斑症を認めた(図 1A)。周辺網膜に明らかな異常はなかった。

蛍光眼底造影検査では黄斑変性に一致した斑状の過螢光を認めた。石原式色覚検査では全色盲を示した。ゴールドマン型動的視

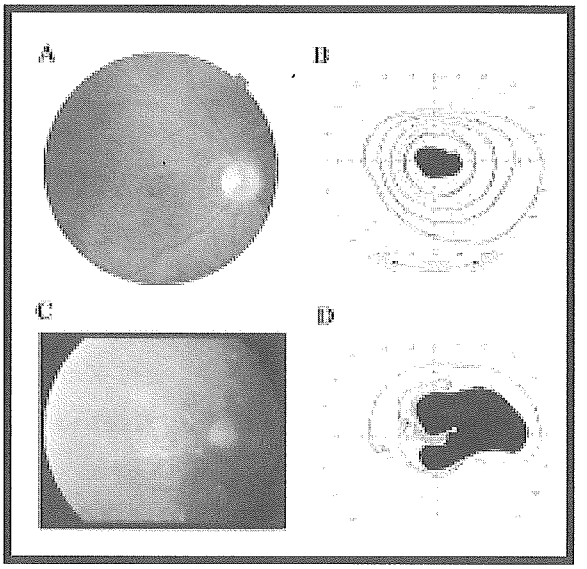

図 1. GUCY2D 遺伝子変異患者の眼底写真 (A、 C) と ゴールドマン動的視野 (B、D) 。 (A、 B) 発端者の右眼、(C、D) 父親の右眼。

野検査では中心 10-20 度の中心暗点を認めた(図 1B)。発端者の全視野錐体 ERG および 30Hz フリッカーERG では反応は消失していた。桿体 b 波の振幅は有意に減少し、白色閃光刺激桿体錐体 ERG の a-、b-波、律動様小波の振幅の低下が認められた。

発端者の 76 歳の父親はより重症であった。矯正視力は右 0.01、左 0.02 で、両眼底黄斑部は網脈絡膜萎縮を生じ、視野検査上中心暗点を認めた(図 1C、D)。蛍光眼底造影では網脈絡膜萎縮を示す低螢光領域を黄斑部に認めた。低視力のため、父親の石原色覚表とパネル D-15 による検査は施行不可能であった。ERG 所見は発端者と類似していたが、振幅はより低下していた(図 4)。

家系内の 2 名の健常者とも両眼矯正視力 1.0 以上で、眼科的に特記すべき異常を認めなかった。

Gene Name	Exon	Nucleotide	Amino acid
AIPL1	2	G268C	D90H
GUCY2D	2	G154T	A52S
GUCY2D	10	C2101T	P701S
RPGRIP1	4	A574G	K192E
RPGRIP1	IVS6-17	907-17 del TAA	SPLICE

表 1　チップ解析で同定された塩基変化

チップおよび遺伝子解析

本家系の典型的な 3 世代にわたる常染色体優性遺伝形式より、adCORD の原因遺伝子検索をおこなった。LCA の原因遺伝子のうち AIPL1、CRX、 GUCY2D は adCORD の原因でもあるため、LCA チップを CORD の原因同定のための初期スクリーニングツールに用いてみることにした。

チップを用いた遺伝子型タイピングにより 5 つのヘテロ接合性の塩基変化を同定した(表 1)。そのうち 1 つが GUCY2D の 2101C>T (P701S) 変化で、すでにホモ接合性変異の場合 LCA となることが報告されているため[3]、GENORAMA ソフト (図 1B) による解析では原因遺伝子変異であると抽出された。残りの 4 つの塩基変化は同ソフトにより遺伝子多型であるとされた。全ての 5 つの塩基変化が正しいことを直接塩基配列決定法により確認した。

GUCY2D の塩基変化が 2 個存在し、

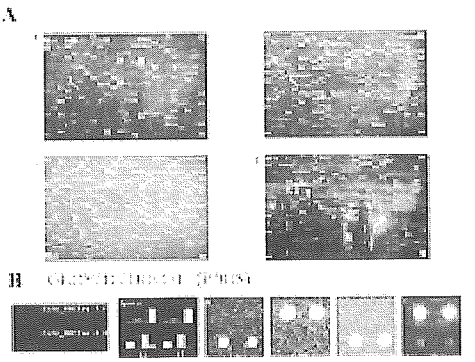

図 2.　発端者の APEX 法を用いた遺伝子型タイピング。(A) 蛍光ラベルしたジデオキシヌクレオチドによるグレースケールイメージ。 (B) GENORAMA ソフトウェアによる GUCY2D コドン 701 の 3 番目の塩基解析。

GENORAMA ソフトでは原因遺伝子であると抽出されたため、我々は次に全ての GUCY2D の遺伝子コード領域の塩基配列を決定した。Gln847Leu と Lys848Gln のアミノ酸変異をもたらす 2540A>T、2541G>C、2542A>C の 3 塩基の連続したヘテロ接合性のミスセンス変異を認めた。これらの変化は発端者と罹患者である父親にのみ認めた

(図 3A)。しかし非罹患者である母親と妹には認められなかった。

これらの 3 つのナンセンス変異が同一の染色体上にあるか両染色体に分散しているかを検討するため、エキソン１３の PCR 産物を TOPO2 ベクターにサブクローニングし、各クローンの塩基配列を決定した。

検証した 8 つのクローンのうち 5 つのクローンが 3 つの塩基変化を全て含んでいたのに対し(図 3C)、残りの 3 つのクローンはワイルドタイプの塩基変化を示した(図 3B)。従って、3 つの連続した塩基変化は単一のアリルに存在することが明らかになった。

D．考察

我々は日本人 adCORD 家系において GUCY2D 遺伝子の新規の連続したミスセンス変異を同定した。 GUCY2D 遺伝子は視細胞特異的な酵素である網膜のグアニル酸シクラーゼ（RetGC-1）をコードし、光トランスダクションカスケードに関与する。

その機能は網膜の 5'-guanosine monophosphate(GMP)から cyclic guanosine monophosphate (cGMP)を合成し、暗順応過程において開大した cGMP 依存性チャネルの比率を増す。

これまで、コドン 838 のヘテロ接合性の変異が好発変異部位であることが明らかとなっているが、我々の研究はコドン 838 以外の GUCY2D 遺伝子の変異が CORD の原因となりうることを確認した。[6]

RetGC-1 はダイマーの状態で存在すると考えられているが、本研究で明らかとなったコドン 847 と 848 の変異部位も RetGC-1 蛋白の重合化部位に存在する。さらにヒト RetGC-1 とそのホモログ (ヒト RetGC-1 、

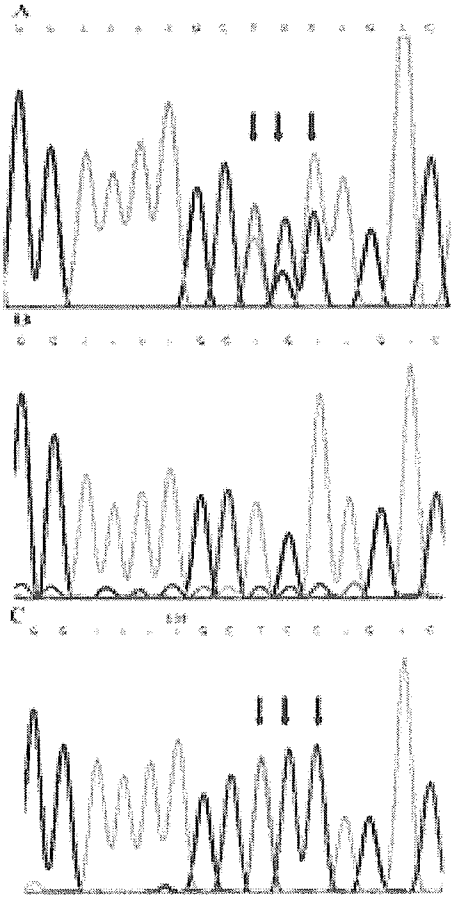

図 5. (A)発端者と父親の GUCY2D 遺伝子のセンス方向の塩基配列。エキソン 13 に 2540A>T、 2541G>C、 2542A>C (Gln847Leu と Lys848Gln)の複合ミスセンス変異を認める。矢印は変異部位を示す。(B) 当該変異は発端者の健常な母と妹では認められない。発端者遺伝子エキソン 13 のサブクローンの塩基配列は正常である。(C) 同一患者の遺伝子エキソン 13 の他のサブクローンの塩基配列は 3 つのミスセンス塩基配列を全て含んでいる。

RetGC-2 、 ラット GC-E 、 GC-F 、 マウス GC-E、牛 ROS-GC) のアラインメント解析ではコドン 848 と 847 は高度に保存されていた。これらの知見は両変異部位とも病態形成に重要であることを示唆している。

我々の研究は 1 度の検査で原因遺伝子変異のみならず疾患修飾遺伝子を同定できる可能性があるという点において、遺伝子型タイピングチップの有用性を提示したと思われる。C2174T (P701S)のヘテロ接合性変化は健常コントロールでも認められたため、本家系では原因遺伝子変異ではないと考えられるが、2540A>T、2541G>C、 2542A>C の主要な変異を有する状態では C2174T の変化は臨床病型の修飾因子となる可能性がある。なぜなら、ホモ接合性の C2174T 変異は LCA の原因となりうるからである。同様に、AIPL、 GUCY2D、RPGRIP1 中に認められた他の 4 つの遺伝子変化も健常人では異常をもたらさなくても他に視細胞に重大な機能障害をもたらす遺伝子変異を有する状態では、疾患修飾遺伝子となりうる可能性がある。さらには多数の遺伝子変異を同時に検証できる本技術は 2 遺伝子性あるいは多遺伝子性の CORD の原因遺伝子を効果的に同定できるツールとなりうる可能性がある。

LCA と CORD 患者の GUCY2D の変異分布が異なり、おそらく日本人 CORD 患者の変異分布は白人のそれと異なるため、本研究ではチップスクリーニングでは原因遺伝子を同定できなかった。しかし、5 つの塩基変化全てが直接塩基配列法で再確認されたため、APEX 法に基づいた遺伝子変異スクリーニングそれ自体は遺伝子型を同定するための正確で効率的な方法となりうると考えられる。[3]

E. 結論

LCA チップの使用中に、我々は、GUCY2D 遺伝子中に新規のヘテロ接合性の変異を同定した。

F. 健康危険情報

なし

G. 研究発表

1. 論文発表

なし

2. 学会発表

なし

H. 知的財産権の出願・登録状況

1. 特許取得

なし

2. 実用新案登録

なし

3. その他

なし

I. 参考文献

1. Mockler TC, et al: Applications of DNA tiling arrays for whole-genome analysis. Genomics 85: 1-15, 2005.
2. Kurg A, et al: Arrayed primer extension: solid-phase four-color DNA resequencing and mutation detection technology. Genet Test 4: 1-7, 2000.
3. Zernant J, et al: Genotyping microarray (disease chip) for leber congenital amaurosis: detection of modifier alleles. Invest Ophthalmol Vis Sci 46: 3052-3059, 2005.
4. Yoshida S, et al: Rapid genotyping for most common TGFBI mutations with real-time polymerase chain reaction.

Hum Genet 116: 518-524, 2005.
5. Yoshida S, et al: Role of MCP-1 and MIP-1alpha in retinal neovascularization during postischemic inflammation in a mouse model of retinal neovascularization. J Leukoc Biol 73: 137-144, 2003.
6. Ito S, et al: Novel complex GUCY2D mutation in Japanese family with cone-rod dystrophy. Invest Ophthalmol Vis Sci 45: 1480-1485, 2004.

Hum Genet (2005) 116: 518–524
DOI 10.1007/s00439-005-1269-0

ORIGINAL INVESTIGATION

Shigeo Yoshida · Yoko Yamaji · Ayako Yoshida · Yoshihiro Noda · Yuji Kumano · Tatsuro Ishibashi

Rapid genotyping for most common *TGFBI* mutations with real-time polymerase chain reaction

Received: 24 November 2004 / Accepted: 5 January 2005 / Published online: 3 March 2005

Abstract Recent studies of the corneal dystrophies (CDs) have shown that most cases of granular CD, Avellino CD, and lattice CD type I are caused by mutations in the human transforming growth factor beta-induced (*TGFBI*) gene. The aim of this study was to develop a rapid diagnostic assay to detect mutations in the *TGFBI* gene. Sixty-six patients from 64 families with *TGFBI*-associated CD were studied. A primer probe set was designed to examine the genome from exons 4 and 12 of the *TGFBI* gene in order to identify mutant and wild-type alleles. A region spanning the mutations was amplified by the polymerase chain reaction (PCR) in a commercial cycler. Mutations were then identified by melting curve analysis of the hybrid formed between the PCR product and a specific fluorescent probe. Using this system, we clearly distinguished each CD genotype (homozygous and heterozygous 418G → A, heterozygous 417C → T, heterozygous 1710C → T, and wild-type) of all the patients by means of the clearly distinct melting peaks at different temperatures. One thermal cycling took approximately 54 min, and all results were completely in concordance with the genotypes determined by conventional DNA sequencing. Thus, the technique is accurate and can be used for routine clinical diagnosis. We expect that our new method will help in making precise diagnoses of patients with atypical CDs and aid the revision of the clinical classification of inherited corneal diseases based on the genetic pathogenesis.

S. Yoshida (✉) · Y. Yamaji · A. Yoshida
Y. Noda · T. Ishibashi
Department of Ophthalmology,
Graduate School of Medical Sciences,
Kyushu University,
Fukuoka 812-8582, Japan
E-mail: yosida@med.kyushu-u.ac.jp
Tel.: +81-92-6425648
Fax: 81-92-642-5663

Y. Kumano
Ohshima Hospital of Ophthalmology, Fukuoka 812-0036, Japan

Introduction

Recent molecular genetic analyses of the corneal dystrophies (CDs) have shown that most cases of granular CD (GCD; OMIM 121900), Avellino CD (ACD; OMIM 607541), and lattice CD type I (LCD I; OMIM 122200) are caused by amino acid substitutions within the transforming growth factor beta-induced (*TGFBI*) gene. This gene encodes the protein keratoepithelin and is located on the long arm of chromosome 5 (5q31; Klintworth 2003; Mashima et al. 2000; Munier et al. 1997; Yamamoto et al. 2000).

Reports from researchers from several countries have shown that the R555W and R124H mutations are the most common cause of GCD and ACD, respectively. For these two dystrophies, the incidence of the R124H mutation-associated ACD phenotype is reported to be the most common at approximately 90% (Fujiki et al. 2001; Mashima et al. 2000). In Caucasians, on the other hand, the GCD phenotype caused by the R555W mutation is the most common (Korvatska et al. 1998; Munier et al. 1997). In contrast, the LCD I has thus far been almost exclusively associated with the R124C mutation in the *TGFBI* gene (Korvatska et al. 1998; Mashima et al. 1997; Mashima et al. 2000; Munier et al. 1997).

Thus, codons R124 and R555 of the *TGFBI* gene are considered to be mutational hotspots in patients with *TGFBI*-associated CDs. We have demonstrated that mutational analysis of these two mutational hotspots in exons 4 and 12 of the *TGFBI* gene provides sufficient information for an initial screening for these CDs (Yoshida et al. 2002a).

Although a clear genotype/phenotype correlation is generally thought to be associated with the *TGFBI* gene (Korvatska et al. 1998; Munier et al. 1997), the clinical manifestation of the same mutation in the *TGFBI* gene can vary, probably modified by the stage of the disease, environmental factors, other gene modifiers, and/or surgical interventions (Chau et al. 2003; El-Ashry et al.

2004; Konishi et al. 1999; Meallet et al. 2004; Morishige et al. 2004; Yoshida et al. 2004b). For example, the R124C mutation is also responsible for "gelatino-lattice" CD whose clinical phenotype resembles gelatinous drop-like CD (Nakamura et al. 2000). We have also reported a case of LCD I without typical lattice lines (Yoshida et al. 2004b). In addition, the more severe phenotypes of GCD and ACD are caused by homozygous mutations in the *TGFBI* gene (Mashima et al. 1998; Okada et al. 1998; Okada et al. 2000), and recurrences of corneal opacities after keratoplasty or phototherapeutic keratectomy limits the recovery of visual acuity (Inoue et al. 2001, 2002). These observations suggest that the molecular genetic analyses of the *TGFBI* gene should be quick and accurate so that the diagnosis of patients with atypical or ambiguous corneal appearance can be rapidly made. This will then allow early consultation regarding the risk and prognosis to patients and their family members (Afshari et al. 2001; Yoshida et al. 2004b).

The molecular genetic analysis of mutations associated with CDs can be performed by several techniques. These include direct genomic sequencing and polymerase chain reaction (PCR)-restriction fragment length polymorphism (RFLP) analyses in which gel electrophoresis makes the isolation laborious and time-consuming. Therefore, the development of a simpler and faster method, which must also be accurate, for the detection of mutations in the *TGFBI* gene would be valuable.

The LightCycler (Roche Diagnostics), which has been available for many years, is a combined microliter volume thermal cycler with an integrated fluorometer (Gotting et al. 2004; Yoshida et al. 2003a, 2003b). It offers a high-throughput semi-automatic method, which allows fast genotyping of mutational sites. The detection of mutations by melting curve analysis is based on the detection of two adjacent oligonucleotide fluorescent probes. One of the probes is a tightly bound anchor probe, and the adjacent detection probe spans the region of the mutation. The detection of the mutation is performed by a post-amplification melting curve analysis of the final PCR products. Sequence alterations are detected by a change in the melting temperature of the detection probe. For a typical homozygous wild-type sample, a single melting peak is observed, and for mixed alleles, two peaks are obtained. In a homozygous mutated sample, a single peak at a temperature different from the wild-type allele is found.

We have succeeded in developing a method to detect mutations in the *TGFBI* gene rapidly. We have optimized a real-time PCR protocol for detecting mutations in the R124 and R555 mutational hot spots and have determined their characteristic melting behavior with the use of sequence-specific fluorescence-labeled hybridization probes.

Materials and methods

Patients and collection of DNA samples

This study was approved by the Ethics Committee of the Ohshima Hospital of Ophthalmology. All patients gave their informed consent prior to participation.

We studied 66 patients from 64 Japanese families with CDs attributable to mutations in the *TGFBI* gene. We have previously reported 45 of these patients from 44 families who were heterozygous for the R124H, R124L, or R555W mutations (Yoshida et al. 2002a); they were reanalyzed for this study. This group included 20 men and 46 women, ranging in age from 16–86 years (mean age: 63.2 ± 15.7 years).

DNA sequence analysis

DNA was extracted from the blood of the 66 CD patients with the QIAamp DNA Blood Mini Kit (QIAGEN, Hilden, Germany) and was used to screen for genetic mutations as described (Yoshida et al. 2002a, 2002b; 2004a, 2005). The genomic DNAs of exons 4 and 12 of the *TGFBI* gene were amplified with appropriate forward and reverse primers (Table 1; exon 4: *TGFBI*4F and *TGFBI*4R; exon 12: *TGFBI*12F and *TGFBI*12R). The conditions for PCR for both exons 4 and 12 were: 10 min at 94°C, followed by 35 cycles of 30 s at 72°C, 94°C for 30 s, and 60°C for 30 s, with a final extension step at 72°C for 5 min. The PCR products were purified and sequenced by using the Big Dye Terminator sequencing kit (Perkin-Elmer Applied Biosystems, Foster City, USA). The

Table 1 Primer and hybridization probe sequences used

Primers/probes	Sequence (5′–3′)
Primers	
*TGFBI*4F	CCCCAGAGGCCATCCCTCCT
*TGFBI*4R	CCGGGCAGACGGAGGTCATC
*TGFBI*12F	GGACTGACGGAGACCCTCAA
*TGFBI*12R	GCATCTCCCAAGAGTCTGCT
Hybridization probes	
*TGFBI*4Flu	CGAGACCCTGGGAGTCGTTGGATCCACCACCACTCAGCT-fluorescein
*TGFBI*4LCRed	LCRed640-ACACGGACCGCACGGA-phosphorylation
*TGFBI*12Flu	CAGTCTTTGCTCCCACAAATGAAGCCTTCCGAGCCCTGCCA-fluorescein
*TGFBI*12LCRed	LCRed640-CAAGAGAACGGAGCAGACT-phosphorylation

products were resolved on an ABI Prism 3100 sequencer (Perkin-Elmer Applied Biosystems).

LightCycler PCR

The PCR and melting curve analyses were performed on the LightCycler (Roche Diagnostics, Mannheim, Germany), which can simultaneously measure the emitted signals from two different fluorophores. The system is equipped with a 470-nm light-emitting diode and has other detection channels at 530, 640, and 710 nm that monitor 32 capillaries simultaneously (Bernard et al. 1998; Kyger et al. 1998; Lay et al. 1997; von Ahsen et al. 1999).

Schematic diagrams of the LightCycler hybridization analysis used in our assay are shown in Fig. 1. The primers and hybridization probes were designed by using LightCycler Probe Design software (Roche Diagnostics) and are shown in Table 1. The detection probes covering the nucleotides at position 417 and 418 (*TGFBI*4LCRed) and at 1710 (*TGFBI*12LCRed) were

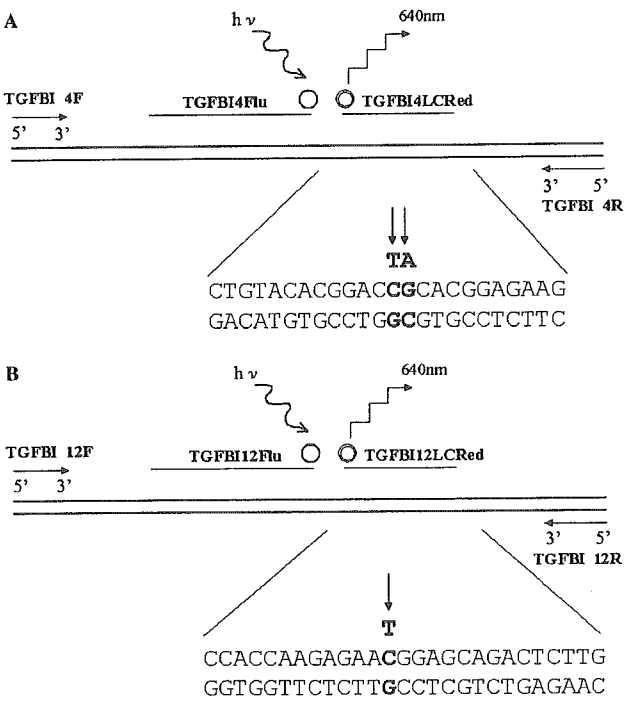

Fig. 1 Schematic illustration of PCR primers, anchors, and detection probes for the *TGFBI* gene (accession no. AY149344). The probes for *TGFBI*4Flu (**a**) and *TGFBI*12Flu (**b**) are labeled with fluorescein at their 3′-end and serve as anchor probes for *TGFBI*4LCRed and *TGFBI*12LCRed, respectively. The detection probes, *TGFBI*4LCRed and *TGFBI*12LCRed, are labeled with LCRed640 at their 5′-end and span the DNA region having the mutations. The pair of anchors and detection probes hybridizes to the template DNA, with a 1-bp gap between them. The region of the mutations of the *TGFBI* gene is shown *below*, and the mutation sites corresponding to 417C → T, 418G → A, and 1710C → T are shown in *bold* and are indicated by *arrows* (→ fluorescein, ← LC-Red 640)

5′-labeled with LightCycler (LC) Red 640 and phosphorylated at the 3′-end (Nippon Gene Research Laboratories, Sendai, Japan). The corresponding anchor probes, *TGFBI*4Flu and *TGFBI*12Flu, respectively, were fluorescein-labeled at the 3′-end (Nippon Gene Research Laboratories). The pair of anchors and detection probes hybridized to the template DNA, with a 1-bp gap between them.

When the probes hybridize to the same DNA strand internal of the PCR primers, the probes come in close proximity to each other and produce a fluorescence resonance energy transfer (FRET). During FRET, a donor fluorophore, which is excited by the LED light source, transfers its energy to an acceptor fluorophore only when it is positioned in the direct vicinity of the former. After a complete PCR run, a melting point analysis can be carried out, during which the temperature is lowered below the annealing temperature for the probes and then slowly increased. The fluorescence signal decreases when the detection probe melts off its target.

The reaction mixtures were prepared in glass capillaries containing 0.5 µl purified genomic DNA, 0.2 µM each primer, 0.2 µM each probe, and 10× Lightcycler Fast Start DNA Master Hybridization Probes mix, and processed according to the manufacturer's instructions (Roche Diagnostics). Real-time PCR was performed by an initial denaturation at 95°C for 10 min, followed by 40 cycles of 95°C for 10 s, 60°C for 15 s, and 72°C for 9 s. Following the amplification phase, a melting curve analysis was performed at 40°C for 20 s, followed by slow heating at 0.2°C/s to 85°C to determine the melting point values by monitoring the reporter dye fluorescence emission in channel F2/F1 (640 nm).

Melting curves were converted into melting peaks by plotting the negative derivative of the fluorescence signal against temperature. The sudden drop in fluorescence signal was thereby transformed to a peak, allowing the easy identification of the Tm mismatches between the hybridization probe and the target.

Results

We had found earlier that mutational analysis of exons 4 and 12 of the *TGFBI* gene, which are the mutational hot spots, provide enough information for a diagnosis during an initial screening (Yoshida et al. 2002a). Direct sequencing of exons 4 and 12 of the *TGFBI* gene in our 66 patients with a clinical diagnosis of CD showed that the patients could be divided into four known mutation genotypes; two homozygous R124H (418G → A), 51 heterozygous R124H (418G → A), five heterozygous R124C (417C → T), and eight heterozygous R555W (1710C → T) mutations.

To develop a reliable and rapid method of genotyping based on the hybridization probe assays, two sequence-

specific primers and fluorophore-labeled probes for exons 4 and 12 of the *TGFBI* gene were designed (Table 1, Fig. 1). The LightCycler was standardized by analyzing the sequence-verified DNA from the 66 *TGFBI*-associated CD patients. With this technique, we were able to distinguish each CD genotype of all the patients by the melting peaks (Fig. 2). Homozygous wild-type (418GG) showed a single peak at 66.0°C. The G/A mismatch at nucleotide 418 (418GA) decreased the Tm with a heterozygous pattern of two peaks at 66.0°C and 59.0°C. The single peak at 59.0°C indicated a homozygous mutation (418AA). Similarly, the C/T mismatch at nucleotide 417 (417CT) showed a heterozygous pattern with two peaks at 66.0°C and 54.5°C, which was clearly distinguishable from the heterozygous 418G → A genotype (Fig. 2a).

Similarly, the 1710 C → T mutation was detected with the specific primers (Table 1). The melting curve of 1710CC showed a homozygous wild-type pattern with a single peak at 64.0°C. The C/T mismatch (1710CT) showed a heterozygous pattern with two peaks at 64.0°C and 54.5°C (Fig. 2b).

One thermal cycling required approximately 54 min. All DNA samples were examined for both exons 4 and 12 under the same PCR conditions in triplicate, and all results were completely in concordance with the genotypes determined by DNA sequencing. We observed little intra-assay and inter-assay variation, and neither shifts of the hybridization probe melting temperatures nor inaccurate melting

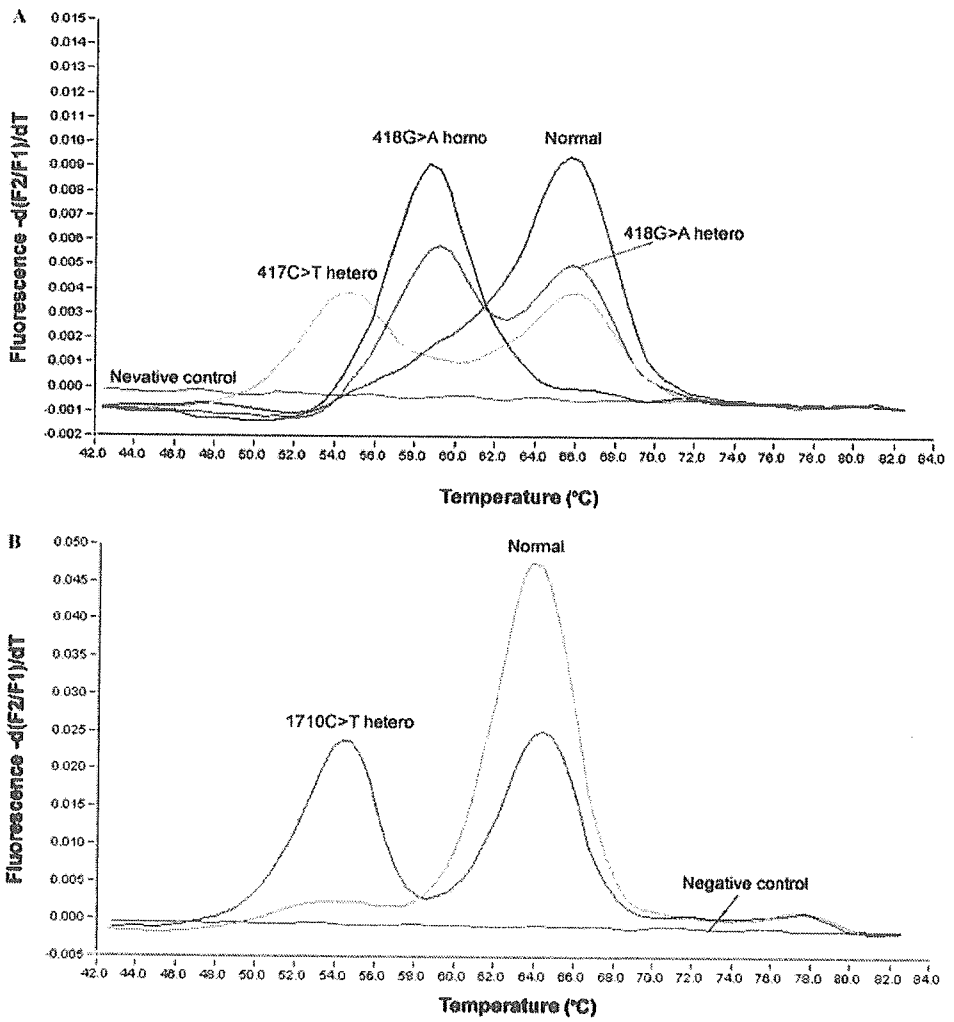

Fig. 2 Real-time genotyping of the *TGFBI* gene around nucleotides 417, 418 (**a**), and 1710 (**b**) by hybridization probe melting curve analysis. Analysis was performed by plotting the first negative derivative of the fluorescence with respect to temperature [−(d *F*/d *T*) versus *T*]. **a** The melting peak temperatures obtained from the derivative melting curves for the 418G → A genotypes are 66.0°C for the homozygous wild-type (GG), 66.0°C and 59.0°C for the heterozygous type (GA), and 59.0° C for the homozygous mutated type (AA). The melting temperature for the heterozygous 417C → T genotypes are 66.0°C and 54.5°C. **b** The melting temperatures for the 1710C → T genotypes are 64.0°C for the homozygous wild-type (CC) and 64.0°C and 54.5°C for the heterozygous type (CT). Genotypes are indicated on *top* of each peak

curves of individual samples were observed (data not shown).

Discussion

We have developed a rapid PCR-based fluorescein assay for the detection of the 418G → A, 417C → T, and 1710C → T mutations in the *TGFBI* gene, i.e., for the mutational hotspots in *TGFBI*-associated CD. The precision of the assays was 100%, demonstrating the complete reproducibility and reliability of our new high-speed genotyping assay.

One of the conventional methods that have been used to detect mutations in patients with CD is based on direct genomic sequencing. Although providing more data, the method is more labor-intensive and expensive. Another method, the PCR-RFLP assay for detecting the 418G → A, 417C → T, and 1710C → T genotypes, requires a PCR amplification of each exon followed by digestion with a mutation-specific restriction enzyme of the amplicons and then gel electrophoresis. Both methods take several hours and require extensive manual interference, resulting in a higher risk of contamination by displaced amplicons. In contrast, our rapid PCR-based fluorescein assay is a closed-tube system with a minimal risk of contamination, yields reliable genotyping results in less than 54 min, and is suitable for routine clinical use. Moreover, our new assay is easily adaptable to other inherited eye diseases that have mutational hot spots, and for large-scale association studies for multifactorial diseases, such as age-related macular degeneration (McKay et al. 2004) and glaucoma.

The clustering of two mutational hot spots that sit next to each other (417C → T and 418G → A) within the human genome facilitates the design of just one probe for mutation detection for both mutations. Because the R124H and R124C mutations account for approximately 90% of Japanese patients with *TGFBI*-associated CDs, this single probe set can detect the most common mutations in the *TGFBI* gene simultaneously and is thus particularly useful and suitable for a rapid initial screening in our clinic. In addition to R124H and R124C, the assays for the 1710C → T mutation can be run simultaneously on one LightCycler by using identical cycling parameters, thereby enabling a screening covering the majority of major mutations in the *TGFBI* gene.

Although this method is useful, one step requires further optimization. Two rare types of CDs, viz., Reis-Bücklers CD (OMIM 608470) and Thiel-Behnke CD (OMIM 602082), are also known to be caused by mutations in the *TGFBI* gene at codon 124 (418G → T) and 555 (1711G → A), respectively. Although we expect that the specific mutations for these diseases can be detected by our assay, we have not been able to obtain blood samples from relevant patients. We are currently recruiting more patients with CDs in order to obtain DNAs from patients with these forms of CD to determine whether those genotypes can be discriminated by our assay.

Increasing numbers of rare gene mutations, such as L518P (Endo et al. 1999; Hirano et al. 2000), L527R (Fujiki et al. 1998, 2000; Hirano et al. 2001), A546D (Aldave et al. 2004a; Eifrig et al. 2004; Klintworth et al. 2004), P551Q (Aldave et al. 2004b; Klintworth et al. 2004), L569R (Warren et al. 2003), or H626R (Afshari et al. 2001; Chau et al. 2003; Dighiero et al. 2001; Ellies et al. 2002), have recently been reported and identified as being associated with mutations in the *TGFBI* gene. These findings indicate that a broader spectrum of disease phenotypes for CDs probably exists than previously believed. Thus, to state with relative certainty that, for example, a *TGFBI*-associated CD has been excluded in a patient with what appears to be corneal amyloid deposits, the previously reported *TGFBI* mutations associated with variants of LCD must be excluded. Obviously, the screening of only codons 124 and 555 would not exclude the majority of the *TGFBI* gene mutations associated with stromal amyloid deposits. Nonetheless, our method will help in identifying those CDs associated with atypical *TGFBI* mutation by use of conventional mutation screening methods, after a rapid and reliable exclusion of the frequent mutations in the *TGFBI* gene. Our technique will also aid the more precise diagnosis and risk prediction of CDs in patients with clinically ambiguous corneal appearance and exclude the possibility of the major types of *TGFBI*-associated CDs in patients with corneal diseases resembling CDs. Finally, we expect that our new method will accelerate the revision of the clinical classification of inherited corneal diseases based not on clinical phenotype but on genetic analyses.

Acknowledgements This work was supported in part by grants from the Ministry of Education, Science, Sports, and Culture of Japan (T.I. and S.Y.), the Clinical Research Foundation (S.Y.) and the Japanese National Society for the Prevention of Blindness (S.Y.).

References

Afshari NA, Mullally JE, Afshari MA, Steinert RF, Adamis AP, Azar DT, Talamo JH, Dohlman CH, Dryja TP (2001) Survey of patients with granular, lattice, avellino, and Reis-Bucklers corneal dystrophies for mutations in the BIGH3 and gelsolin genes. Arch Ophthalmol 119:16–22

Ahsen N von, Schutz E, Armstrong VW, Oellerich M (1999) Rapid detection of prothrombotic mutations of prothrombin (G20210A), factor V (G1691A), and methylenetetrahydrofolate reductase (C677T) by real-time fluorescence PCR with the LightCycler. Clin Chem 45:694–696

Aldave AJ, Gutmark JG, Yellore VS, Affeldt JA, Meallet MA, Udar N, Rao NA, Small KW, Klintworth GK (2004a) Lattice corneal dystrophy associated with the Ala546Asp and Pro551Gln missense changes in the TGFBI gene. Am J Ophthalmol 138:772–781

Aldave AJ, Yellore VS, Self CA, Holsclaw D, Small K (2004b) The usefulness of buccal swabs for mutation screening in patients with suspected corneal dystrophies. Ophthalmology 111:1407–1409

Bernard PS, Lay MJ, Wittwer CT (1998) Integrated amplification and detection of the C677T point mutation in the methylenetetrahydrofolate reductase gene by fluorescence resonance energy transfer and probe melting curves. Anal Biochem 255:101–107

Chau HM, Ha NT, Cung LX, Thanh TK, Fujiki K, Murakami A, Kanai A (2003) H626R and R124C mutations of the TGFBI (BIGH3) gene caused lattice corneal dystrophy in Vietnamese people. Br J Ophthalmol 87:686–689

Dighiero P, Niel F, Ellies P, D'Hermies F, Savoldelli M, Renard G, Delpech M, Valleix S (2001) Histologic phenotype-genotype correlation of corneal dystrophies associated with eight distinct mutations in the TGFBI gene. Ophthalmology 108:818–823

Eifrig DE Jr, Afshari NA, Buchanan HWt, Bowling BL, Klintworth GK (2004) Polymorphic corneal amyloidosis: a disorder due to a novel mutation in the transforming growth factor beta-induced (BIGH3) gene. Ophthalmology 111:1108–1114

El-Ashry MF, Abd El-Aziz MM, Ficker LA, Hardcastle AJ, Bhattacharya SS, Ebenezer ND (2004) BIGH3 mutation in a Bangladeshi family with a variable phenotype of LCDI. Eye 18:723–728

Ellies P, Renard G, Valleix S, Boelle PY, Dighiero P (2002) Clinical outcome of eight BIGH3-linked corneal dystrophies. Ophthalmology 109:793–797

Endo S, Nguyen TH, Fujiki K, Hotta Y, Nakayasu K, Yamaguchi T, Ishida N, Kanai A (1999) Leu518Pro mutation of the beta ig-h3 gene causes lattice corneal dystrophy type I. Am J Ophthalmol 128:104–106

Fujiki K, Hotta Y, Nakayasu K, Yokoyama T, Takano T, Yamaguchi T, Kanai A (1998) A new L527R mutation of the betaIGH3 gene in patients with lattice corneal dystrophy with deep stromal opacities. Hum Genet 103:286–289

Fujiki K, Hotta Y, Nakayasu K, Yamaguchi T, Kato T, Uesugi Y, Ha NT, Endo S, Ishida N, Lu WN, Kanai A (2000) Six different mutations of TGFBI (betaig-h3, keratoepithelin) gene found in Japanese corneal dystrophies. Cornea 19:842–845

Fujiki K, Nakayasu K, Kanai A (2001) Corneal dystrophies in Japan. J Hum Genet 46:431–435

Gotting C, Schulz V, Hendig D, Grundt A, Dreier J, Szliska C, Brinkmann T, Kleesiek K (2004) Assessment of a rapid-cycle PCR assay for the identification of the recurrent c.3421C → T mutation in the ABCC6 gene in pseudoxanthoma elasticum patients. Lab Invest 84:122–130

Hirano K, Hotta Y, Fujiki K, Kanai A (2000) Corneal amyloidosis caused by Leu518Pro mutation of betaig-h3 gene. Br J Ophthalmol 84:583–585

Hirano K, Hotta Y, Nakamura M, Fujiki K, Kanai A, Yamamoto N (2001) Late-onset form of lattice corneal dystrophy caused by leu527Arg mutation of the TGFBI gene. Cornea 20:525–529

Inoue T, Watanabe H, Yamamoto S, Inoue Y, Okada M, Hori Y, Maeda N, Hayashi K, Shimomura Y, Tano Y (2001) Different recurrence patterns after phototherapeutic keratectomy in the corneal dystrophy resulting from homozygous and heterozygous R124H BIG-H3 mutation. Am J Ophthalmol 132:255–257

Inoue T, Watanabe H, Yamamoto S, Maeda N, Inoue Y, Shimomura Y, Tano Y (2002) Recurrence of corneal dystrophy resulting from an R124H Big-h3 mutation after phototherapeutic keratectomy. Cornea 21:570–573

Klintworth GK (2003) The molecular genetics of the corneal dystrophies—current status. Front Biosci 8:d687–d713

Klintworth GK, Bao W, Afshari NA (2004) Two mutations in the TGFBI (BIGH3) gene associated with lattice corneal dystrophy in an extensively studied family. Invest Ophthalmol Vis Sci 45:1382–1388

Konishi M, Yamada M, Nakamura Y, Mashima Y (1999) Varied appearance of cornea of patients with corneal dystrophy associated with R124H mutation in the BIGH3 gene. Cornea 18:424–429

Korvatska E, Munier FL, Djemai A, Wang MX, Frueh B, Chiou AG, Uffer S, Ballestrazzi E, Braunstein RE, Forster RK, Culbertson WW, Boman H, Zografos L, Schorderet DF (1998) Mutation hot spots in 5q31-linked corneal dystrophies. Am J Hum Genet 62:320–324

Kyger EM, Krevolin MD, Powell MJ (1998) Detection of the hereditary hemochromatosis gene mutation by real-time fluorescence polymerase chain reaction and peptide nucleic acid clamping. Anal Biochem 260:142–148

Lay MJ, Wittwer CT (1997) Real-time fluorescence genotyping of factor V Leiden during rapid-cycle PCR. Clin Chem 43:2262–2267

Mashima Y, Imamura Y, Konishi M, Nagasawa A, Yamada M, Oguchi Y, Kudoh J, Shimizu N (1997) Homogeneity of keratoepithelin codon 124 mutations in Japanese patients with either of two types of corneal stromal dystrophy. Am J Hum Genet 61:1448–1450

Mashima Y, Konishi M, Nakamura Y, Imamura Y, Yamada M, Ogata T, Kudoh J, Shimizu N (1998) Severe form of juvenile corneal stromal dystrophy with homozygous R124H mutation in the keratoepithelin gene in five Japanese patients. Br J Ophthalmol 82:1280–1284

Mashima Y, Yamamoto S, Inoue Y, Yamada M, Konishi M, Watanabe H, Maeda N, Shimomura Y, Kinoshita S (2000) Association of autosomal dominantly inherited corneal dystrophies with BIGH3 gene mutations in Japan. Am J Ophthalmol 130:516–517

McKay GJ, Clarke S, Hughes A, McConnell V, Schultz DW, Klein ML, Silvestri G, Simpson DA (2004) A novel diagnostic test detects a low frequency of the hemicentin Gln5345Arg variant among Northern Irish age related macular degeneration patients. Mol Vis 10:682–687

Meallet MA, Affeldt JA, McFarland TJ, Appukuttan B, Read R, Stout JT, Rao NA (2004) An unusual clinical phenotype of Avellino corneal dystrophy associated with an Arg124His beta iG-H3 mutation in an African-American woman. Am J Ophthalmol 137:765–767

Morishige N, Chikama T, Ishimura Y, Nishida T, Takahashi M, Mashima Y (2004) Unusual phenotype of an individual with the R124C mutation in the TGFBI gene. Arch Ophthalmol 122:1224–1227

Munier FL, Korvatska E, Djemai A, Le Paslier D, Zografos L, Pescia G, Schorderet DF (1997) Kerato-epithelin mutations in four 5q31-linked corneal dystrophies. Nat Genet 15:247–251

Nakamura T, Nishida K, Dota A, Adachi W, Yamamoto S, Maeda N, Okada M, Kinoshita S (2000) Gelatino-lattice corneal dystrophy: clinical features and mutational analysis. Am J Ophthalmol 129:665–666

Okada M, Yamamoto S, Inoue Y, Watanabe H, Maeda N, Shimomura Y, Ishii Y, Tano Y (1998) Severe corneal dystrophy phenotype caused by homozygous R124H keratoepithelin mutations. Invest Ophthalmol Vis Sci 39:1947–1953

Okada M, Yamamoto S, Watanabe H, Shimomura Y, Tano Y (2000) Granular corneal dystrophy with homozygous mutations in the kerato-epithelin gene. Am J Ophthalmol 129:411–412

Warren JF, Abbott RL, Yoon MK, Crawford JB, Spencer WH, Margolis TP (2003) A new mutation (Leu569Arg) within exon 13 of the TGFBI (BIGH3) gene causes lattice corneal dystrophy type I. Am J Ophthalmol 136:872–878

Yamamoto S, Okada M, Tsujikawa M, Morimura H, Maeda N, Watanabe H, Inoue Y, Shimomura Y, Kinoshita S, Tano Y (2000) The spectrum of beta ig-h3 gene mutations in Japanese patients with corneal dystrophy. Cornea 19:S21–S23

Yoshida S, Kumano Y, Yoshida A, Hisatomi T, Matsui H, Nishida T, Ishibashi T, Matsui T (2002a) An analysis of BIGH3 mutations in patients with corneal dystrophies in the Kyushu district of Japan. Jpn J Ophthalmol 46:469–471

Yoshida S, Kumano Y, Yoshida A, Numa S, Yabe N, Hisatomi T, Nishida T, Ishibashi T, Matsui T (2002b) Two brothers with gelatinous drop-like dystrophy at different stages of the disease: role of mutational analysis. Am J Ophthalmol 133:830–832

Yoshida S, Yoshida A, Ishibashi T, Elner SG, Elner VM (2003a) Role of MCP-1 and MIP-1alpha in retinal neovascularization during postischemic inflammation in a mouse model of retinal neovascularization. J Leukoc Biol 73:137–144

Yoshida S, Yoshida A, Matsui H, Takada Y, Ishibashi T (2003b) Involvement of macrophage chemotactic protein-1 and interleukin-1beta during inflammatory but not basic fibroblast growth factor-dependent neovascularization in the mouse cornea. Lab Invest 83:927–938

Yoshida S, Arita R, Yoshida A, Tada H, Emori A, Noda Y, Nakao S, Fujisawa K, Ishibashi T (2004a) Novel mutation in FZD4 gene in a Japanese pedigree with familial exudative vitreoretinopathy. Am J Ophthalmol 138:670–671

Yoshida S, Yoshida A, Nakao S, Emori A, Nakamura T, Fujisawa K, Kumano Y, Ishibashi T (2004b) Lattice corneal dystrophy type I without typical lattice lines: role of mutational analysis. Am J Ophthalmol 137:586–588

Yoshida S, Honda M, Yoshida A, Nakao S, Goto Y, Nakamura T, Fujisawa K, Ishibashi T (2005) Novel mutation in ABCC6 gene in a Japanese pedigree with pseudoxanthoma elasticum and retinitis pigmentosa. Eye 19:215–217

Eye (2005), 1–2

www.nature.com/eye

Sir,

Novel mutation in exon 2 of *COL2A1* gene in Japanese family with Stickler Syndrome type I

Stickler Syndrome (STL) is an autosomal dominant disorder characterized by degeneration of the vitreous and retina, and is frequently associated with myopia.[1] It is also accompanied by nonocular signs, such as orofacial anomalies, deafness, and arthritis. There are no widely accepted clinical diagnostic criteria for STL in ophthalmology.[2] Based on locus heterogeneity, a subclassification of STL has been proposed; *COL2A1* mutation associated STL type I with a congenital 'membranous' vitreous anomaly; *COL11A1* mutations associated with STL type II showing a 'beaded' phenotype; and *COL11A2* mutations associated with non-ocular STL type III (OMIM 120140, 120280, and 120290).[3] A subgroup of STL type I patients has been identified who are characterized by predominantly ocular disorders without systemic involvement.[4,5] It has been suggested that molecular genetics and scrutiny of the phenotype will provide evidence that clinicians require for accurate diagnosis.[2] However, several cases of STL with different degrees of severity and manifestations, and genetic background, have been reported mainly in the Western world.

Case report

We report on a 25-year-old Japanese woman who was referred to our clinic with a diagnosis of rhegmatogenous retinal detachment of the right eye. Family history revealed that her mother had undergone retinal detachment surgery in her forties. On the initial examination, her best-corrected visual acuity was 20/20 OU, and her refraction was −9.0 diopter sphere (DS) OD eye and −7.5 DS OS. Anterior-segment examination was unremarkable with clear lenses. Vitreous examination confirmed the presence of a type I membranous vitreous anomaly (Figure 1a and b). Ophthalmoscopy showed a horseshoe tear surrounded by a retinal detachment in the right peripheral retina, and circumferentially oriented lattice degenerations in both eyes. Atrophy of the retinal pigment epithelium, choriocapillaris and radial perivascular degeneration were not seen. No systemic abnormalities were found. We performed scleral buckling on the right eye and the detached retina was reattached.

Although we had tentatively diagnosed the proband with predominantly ocular STL type I based on her ocular features, we could not completely exclude other possibilities because of the unknown genetic a etiology of STL in the Eastern world. In addition, the absence of systemic involvement indicated that the patient had not met the criteria for the diagnosis of STL proposed by Snead.[1]

After obtaining informed consent, we performed direct sequencing of all coding regions of the *COL2A1* gene and found a heterozygous deletion of a G at position 237, which predicts a downstream premature stop codon in exon 5 of the *COL2A1* gene (accession number: NM001844) (Figure 2). Her mother, who declined ophthalmic examination, carried the same mutation in the *COL2A1* gene in the heterozygous state. This deletion was not detected in her father and 45 healthy controls.

Comments

Our study adds a novel mutation of the *COL2A1* gene to the existing mutations that causes STL type I. Based on

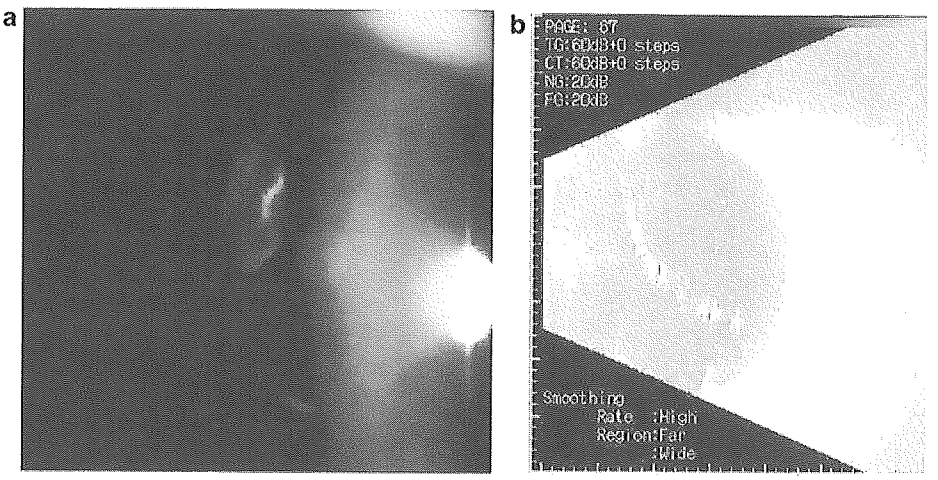

Figure 1 Slit-lamp photograph, ultrasonogram, and fundus photograph of the right eye. (a) Slit-lamp photograph (right eye) of the 25-year-old proband showing type I membranous vitreous anomaly. (b) B-mode ultrasonogram showing membranous vitreous that is set well back in the posterior segment of the right eye.

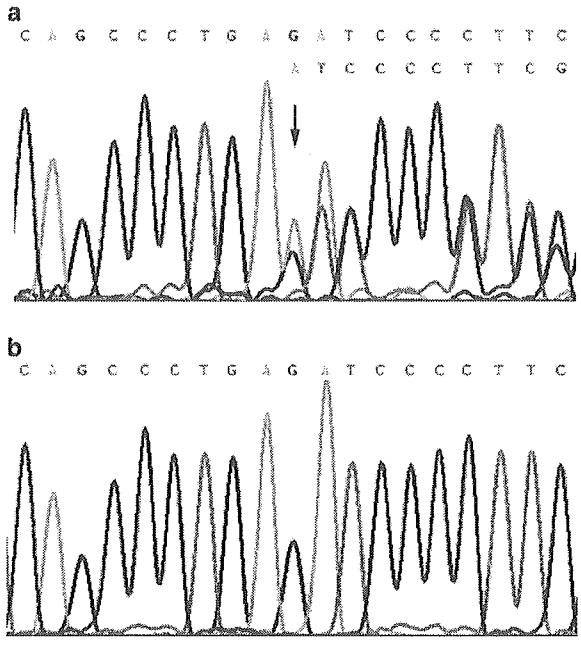

Figure 2 Direct sequence analysis of exon 2 of the *COL2A1* gene. (a) Arrow points to the heterozygous 1 bp deletion in exon 2 of the *COL2A1* gene identified in the proband and her mother which predicts a downstream premature stop codon in exon 5. This may lead to nonsense-mediated decay and haploinsufficiency. (b) No equivalent mutation was detected in her father or control subjects.

the mutational analyses, we counseled our patient that her future children should undergo ophthalmic examinations and molecular analysis for earlier diagnosis or exclusion of STL. Our observations further supported the idea that, irrespective of race, mutations involving exon 2 of the *COL2A1* gene are characterized by a predominantly ocular STL phenotype.[4,5]

The existence of a predominantly ocular type of STL disorder may make an accurate diagnosis of the disease difficult, and the diagnosis of STL may be significantly overlooked in Japan. Although it has been proposed that radial perivascular retinal degeneration is a prominent feature of this predominantly ocular Stickler subset,[6] we did not observe this feature in our patient. Therefore, molecular genetic analysis of the *COL2A1* gene should be considered in routine clinical examination not only for accurate diagnosis of patients with predominantly ocular STL type I, but also for establishing reliable clinical diagnostic criteria.

Acknowledgements

We thank Dr Carel B Hoyng (University Medical Centre Nijmegen, Nijmegen, The Netherlands) for providing primer sequence information of *COL2A1*. This work was supported in part by grants from the Ministry of Education, Science, Sports and Culture, Japan (TI and SY), Japanese Retinitis Pigmentosa Society (SY), Clinical Research Foundation (SY) and Japan National Society for the Prevention of Blindness (SY).

References

1 Snead MP, Yates JR. Clinical and molecular genetics of Stickler syndrome. *J Med Genet* 1999; **36**: 353–359.
2 Parke DW. Stickler syndrome: clinical care and molecular genetics. *Am J Ophthalmol* 2002; **134**: 746–748.
3 Richards AJ, Baguley DM, Yates JR, Lane C, Nicol M, Harper PS *et al.* Variation in the vitreous phenotype of Stickler syndrome can be caused by different amino acid substitutions in the X position of the type II collagen Gly-X-Y triple helix. *Am J Hum Genet* 2000; **67**: 1083–1094.
4 Richards AJ, Martin S, Yates JR, Scott JD, Baguley DM, Pope FM *et al.* COL2A1 exon 2 mutations: relevance to the Stickler and Wagner syndromes. *Br J Ophthalmol* 2000; **84**: 364–371.
5 Donoso LA, Edwards AO, Frost AT, Ritter R, Ahmad NN, Vrabec T *et al.* Identification of a stop codon mutation in exon 2 of the collagen 2A1 gene in a large stickler syndrome family. *Am J Ophthalmol* 2002; **134**: 720–727.
6 Parma ES, Korkko J, Hagler WS, Ala-Kokko L. Radial perivascular retinal degeneration: a key to the clinical diagnosis of an ocular variant of Stickler syndrome with minimal or no systemic manifestations. *Am J Ophthalmol* 2002; **134**: 728–734.

S Yoshida, Y Yamaji, R Kuwahara, A Yoshida, T Hisatomi, A Ueno and T Ishibashi

Department of Ophthalmology, Kyushu University Graduate School of Medical Sciences, Fukuoka 812-8582, Japan

Correspondence: S Yoshida,
Tel: +81 92 642 5648;
Fax: +81 92 642 5663.
E-mail: yosida@med.kyushu-u.ac.jp

Eye advance online publication, 8 July 2005;
doi:10.1038/sj.eye.6702001

2. 日本人 Leber 先天盲の遺伝子変異解析

板橋俊隆、和田裕子、多田麻子、今井詠子、助川真里絵、佐藤　肇、遠藤麻衣、西田幸二
（東北大）

研究要旨　日本人 Leber 先天盲患者に対して、7 種類の原因遺伝子（RPE65, CRX, LRAT, GUCY2D, TULP1, AIPL1, RDH12）を用いて遺伝子解析を行い、日本人 Leber 先天盲における遺伝子変異の頻度及び遺伝子型と表現型との関連を検討した。Leber 先天盲 72 家系を対象とし、PCR-Direct sequence 法により塩基配列を決定した。遺伝子変異を確認した症例については眼科的検索を施行した。

Leber 先天盲 72 家系中 3 家系（5%）に、6 種類の病気の原因となる遺伝子変異を確認した。1 家系の同胞例に RPE65 遺伝子の複合ヘテロ変異を認め、1 家系 1 例に AIPL1 遺伝子の複合ヘテロ変異を認め、1 家系の同胞例に RDH12 遺伝子の複合ヘテロ変異を認めた。7 遺伝子の変異を確認した頻度は、RPE65 遺伝子 1.4%、AIPL1 遺伝子 1.4%、RDH12 遺伝子 1.4% であった。臨床像を検討した結果、これらの 3 例の視力は 0.2～光覚弁であった。AIPL1 遺伝子変異をもつ症例は眼振を伴っており、両眼に重症な網膜変性と円錐角膜を認めた。RPE65 遺伝子変異をもつ症例の 20 年間の臨床経過を観察したところ、網膜変性の進行は緩徐で、周辺視野は保存されていた。

今回我々は、7 種類の原因遺伝子検索を施行し日本人 Leber 先天盲の 5%に遺伝子変異を確認し、RPE65 遺伝子、RDH12 遺伝子、AIPL1 遺伝子は日本人 Leber 先天盲の原因遺伝子になる事が判明したが、遺伝子変異の頻度には人種差が関与していると考えられた。

A．研究目的

Leber 先天盲は、1869 年 Leber により早期発症・重症の遺伝性網膜変性により先天盲を来たす疾患が報告された[1]。その後 Leber 先天盲の原因遺伝子異常が確認され、現在まで 9 種類の原因遺伝子が報告されている。遺伝子異常と共に臨床像との関連も報告されており、Hanein らは遺伝子型と表現型のフローチャートを作成し、原因遺伝子異常により錐体優位に障害される Leber 先天盲を呈する場合と桿体優位に障害される Leber 先天盲を呈する場合がある事を報告している[2]。

今回我々は、日本人 Leber 先天盲患者に対して既報告の原因遺伝子 9 種類のうち 7 種類の遺伝子を用いてスクリーニングを施行し、遺伝子変異の頻度及び遺伝子型と表現型との関連を検討する事を目的とした。

B．研究方法

眼科的検索により Leber 先天盲と診断した 72 家系を対象とした。遺伝子解析にインフォームド・コンセントを得た後、患者の抹消血白血球よりゲノム DNA を抽出した。7 種類の原因遺伝子（RPE65, RDH12, LRAT, GUCY2D, TULP1, AIPL1, CRX）の全翻訳

領域をスクリーニングするためにプライマーを設定し、PCR-Direct sequence 法により塩基配列の決定を行い解析した。

C．研究結果

Leber 先天盲 72 家系中 3 家系（5%）に、6 種類の病気の原因となる遺伝子変異を確認した。Leber 先天盲の同胞例に RPE65 遺伝子の Arg515Trp 変異と Arg124X 変異を複合ヘテロで認め、1 症例では AIPL1 遺伝子の Leu154Pro 変異と 733-735delGAG 変異を複合ヘテロで認めた。RDH12 遺伝子変異解析結果では、Leber 先天盲の同胞例に Lys192X 変異と Gln161Trp 変異を複合ヘテロで認め、家系内調査において表現型との関連を認めた。RPE65 遺伝子 Arg515Trp 変異をヘテロ接合体で 3 家系に認めたが、他アレルに遺伝子変異を認めなかった。7 遺伝子の変異を確認した頻度は、RPE65 遺伝子 1.4%、CRX 遺伝子 0%、LRAT 遺伝子 0%、GUCY2D 遺伝子 0%、CRB1 遺伝子 0%、AIPL1 遺伝子 1.4%、RDH12 遺伝子 1.4%であった。これらの遺伝子変異のうち AIPL1 遺伝子 Leu154Pro と 733-735delGAG、RDH12 遺伝子 Lys192X と Gln161Trp は新規変異であった。遺伝子変異を確認した症例は全例夜盲を認め、そのうち AIPL1 遺伝子変異をもつ症例は眼振を伴っていた。これらの症例の視力は 0.2～光覚弁であった。また AIPL1 遺伝子変異をもつ症例は、両眼に重症な網膜変性と円錐角膜を認めた。RPE65 遺伝子変異をもつ症例の 20 年間の臨床経過を観察したところ、網膜変性の進行は緩徐で、周辺視野は保存されていた。

D．考察

遺伝子解析の結果、我々の研究では Leber 先天盲の 5%に遺伝子異常を確認したが、Hanein らの報告では Leber 先天盲の 47.5%に遺伝子異常を確認したと報告されている[2]。比較すると、日本人 Leber 先天盲患者で遺伝子異常を確認する頻度は非常に低いと考えられた（図 1）。

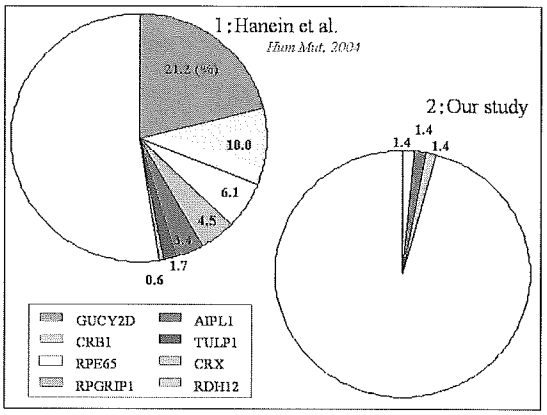

図 1　遺伝子別解析結果の比較
Hanein らの報告では 47.5%、我々の研究では 5.2%に遺伝子異常を確認した。

遺伝子異常を確認した症例の臨床像を検討した結果、RPE65 遺伝子異常及び RDH12 遺伝子異常を認めた症例は桿体優位に障害される Leber 先天盲を呈し、AIPL1 遺伝子異常を認めた症例は錐体優位に障害される Leber 先天盲を呈した。これらのうち RPE65 遺伝子異常と AIPL1 遺伝子異常は Hanein らの報告の表現型と一致した所見が多く認められた[2]。RDH12 遺伝子異常をもつ症例の臨床像は、桿体優位に障害される Leber 先天盲の中でさらに細分化した分類は明確ではなかった（図 2）。

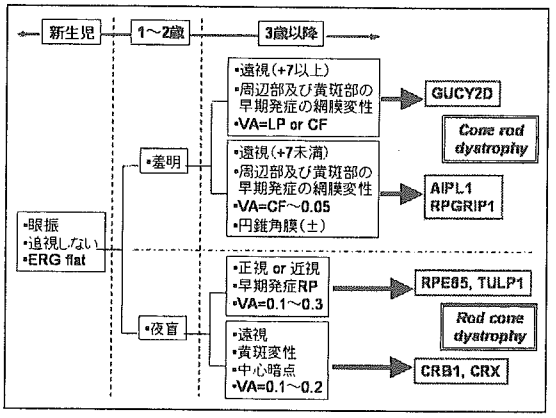

図 2　遺伝子異常をもつ Leber 先天盲患者の臨床像フローチャート（Hanein et al. Hum Mut. 2004 より引用）

E．結論

7 種類の原因遺伝子検索を施行し、日本人 Leber 先天盲の 5%に遺伝子変異を確認した。RPE65 遺伝子、RDH12 遺伝子、AIPL1 遺伝子は日本人 Leber 先天盲の原因遺伝子になる事が判明したが、遺伝子変異の頻度には人種差が関与していると考えられた。

F．健康危険情報

なし

G．研究発表

1．論文発表

なし

2．学会発表

1. 板橋俊隆　他　「日本人常染色体優性網膜色素変性における CA4 遺伝子変異解析」　第 109 回日本眼科学会（2005 年 3 月）
2. 板橋俊隆　他　「遺伝性網膜疾患の遺伝子解析結果と臨床像の検討」　第 59 回日本臨床眼科学会（2005 年 10 月）

H．知的財産権の出願・登録状況

1．特許取得

なし

2．実用新案登録

なし

3．その他

なし

I．参考文献

1. Leber T. Retinitis pigmentosa und angeborene Amaurose. Albrecht von Graefes Arch Ophthal. 15: 1-25, 1869.
2. Hanein S, Perrault I, Gerber S. et al. Leber Congenital Amaurosis: Comprehensive Survey of the Genetic Heterogeneity, Refinement of the Clinical Definition, and Genotype–Phenotype Correlations as a Strategy for Molecular Diagnosis. Hum Mut. 23: 306-317, 2004.

Screening for Mutations in *CYP4V2* Gene in Japanese Patients With Bietti's Crystalline Corneoretinal Dystrophy

YUKO WADA, MD, TOSHITAKA ITABASHI, MD, HAJIME SATO, MD, MIYUKI KAWAMURA, MD, ASAKO TADA, MD, AND MAKOTO TAMAI, MD

• PURPOSE: To describe the clinical and genetic characteristics of six Japanese families with Bietti's crystalline corneoretinal dystrophy (BCD).
• DESIGN: Case reports and results of DNA analysis.
• METHODS: Mutation screening was performed on six unrelated patients with BCD by direct sequencing. The clinical features were characterized by the visual acuity, slit-lamp biomicroscopy, electroretinography, fluorescein angiography, and kinetic visual field testing.
• RESULTS: An identical IVS6 to 8delTCATACAGGTCATCGCG/insGC mutation in the *CYP4V2* gene was identified in five of the patients with BCD; the sixth patient had a novel Trp340X mutation in the *CYP4V2* gene. Three patients showed crystalline-like deposits at the limbus by specular microscopy. Ophthalmic findings of all patients had a rapid progression after age 50 years.
• CONCLUSIONS: Our findings suggest that the IVS6 to 8delTCATACAGGTCATCGCG/insGC mutation is a common mutation in Japanese patients with BCD. Although phenotypic variability was found, the natural course was almost the same in all of our patients. (Am J Ophthalmol 2005;139:894–899. © 2005 by Elsevier Inc. All rights reserved.)

IN 1937, BIETTI[1] FIRST DESCRIBED THREE CASES OF TAPETORETINAL degeneration characterized by yellowish glistening crystals in the retina and tapetoretinal degeneration with choroidal sclerosis and marginal crystalline deposits in the cornea. These cases have been called Bietti's tapetoretinal degeneration with marginal corneal dystrophy, crystalline retinopathy, or Bietti's crystalline corneoretinal dystrophy (BCD).[2,3] Corneal deposits are not observed in all cases with crystalline retinopathy; both Francois and associates[4] and Grizzard and associates[5] described the crystalline retinopathy without the corneal changes.

BCD is a rare retinal dystrophy with an autosomal recessive inheritance pattern; it is relatively more common in Japanese and Chinese. In 2000, it was reported that the locus of the gene for BCD was mapped to 4q35,[6] and in 2004, the *CYP4V2* gene was described to be the causative gene for BCD.[7] The *CYP4V2* gene consists of 11 exons and encodes 525 amino acids. It is a member of the cytochrome P450 gene and is ubiquitously expressed. This gene has been thought to play a role in fatty acid and corticosteroid metabolism.[7]

We report the presence of IVS6 to 8delTCATACAGGTCATCGCG/insGC and Trp340X mutations of the *CYP4V2* gene in six unrelated Japanese patients with BCD and describe the clinical features of these patients.

METHODS

• SUBJECTS AND MUTATION ANALYSIS: After explaining the purpose of this study, informed consent was obtained from all subjects. The procedures conformed to the tenets of the Declaration of Helsinki.

We screened genomic DNA samples isolated from six unrelated patients with BCD for mutations in the *CYP4V2* gene. Genomic DNA was isolated from leukocytes prepared from a sample of each patient's blood (10-15 ml) using the Gene Ball Genome Preparation Kit (TaKaRa, Kyoto, Japan).

The sequences from exon 1 to exon 11 of the *CYP4V2* gene were amplified by polymerase chain reaction with 10 sets of oligonucleotide primer pairs to amplify the entire coding region.[7] The PCR products were sequenced directly with an ABI sequencer (Model 3100; Applied Biosystems, Foster City, California).

• CLINICAL EXAMINATION: The pedigrees of the six unrelated patients with BCD who were examined at the

Accepted for publication Nov 29, 2004.
From the Department of Ophthalmology, Tohoku University School of Medicine, Sendai, Japan.
Inquiries to Yuko Wada, MD, Department of Ophthalmology, Tohoku University School of Medicine, 1-1 Seiryo-machi, Aoba-ku, Sendai 980-77, Japan; Fax: (+81) 22-717-7298; e-mail: yukow@oph.med.tohoku.ac.jp

0002-9394/05/$30.00
doi:10.1016/j.ajo.2004.11.065

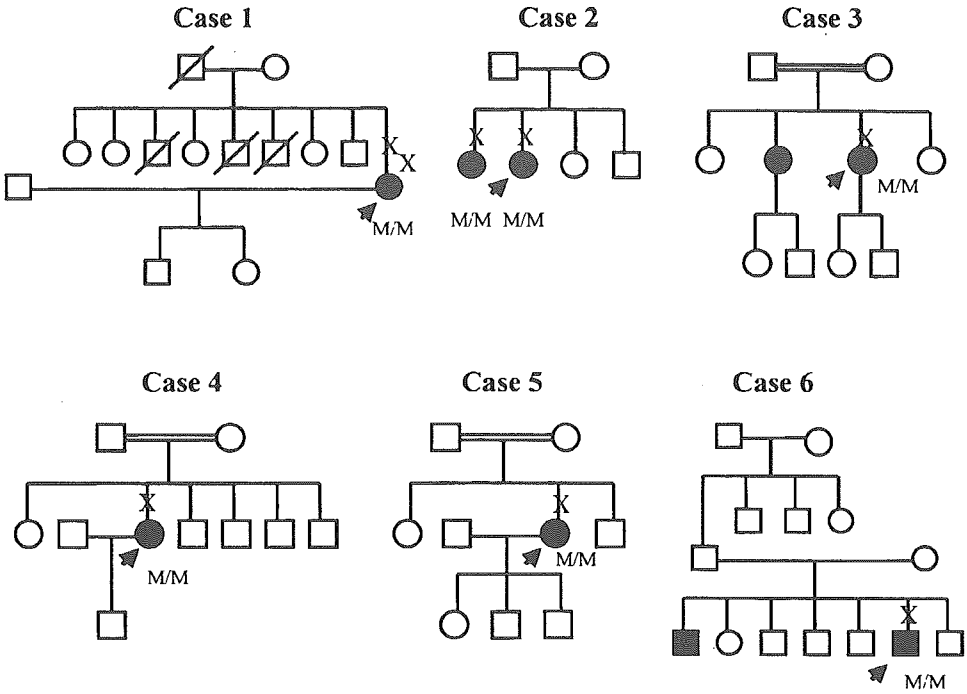

FIGURE 1. Pedigree of six Japanese families with Bietti's crystalline corneoretinal dystrophy associated with the mutations in the *CYP4V2* gene showing affected (solid symbols) and unaffected (open symbols) members. Squares, male members; circles, female members; X, individuals examined in this study; arrow, proband; M, mutant allele; +, normal allelle.

Tohoku University Hospital, Sendai, Japan, are shown in Figure 1. The ophthalmic examination included best corrected visual acuity, slit-lamp biomicroscopy, kinetic visual field testing, fundus examination, fluorescein angiography, and electroretinography (ERGs). Ophthalmoscopic findings were recorded by color fundus photography. The visual field examination was performed on a Goldmann perimeter.

The ERGs were recorded under conditions that conformed to the standards of the International Society of Clinical Electrophysiology of Vision.[8] ERGs were elicited by a single flash or 30-Hz flicker red light under light-adapted conditions for the cone-isolated responses. Rod-isolated responses were elicited by a dim blue flash after 30 minutes of dark adaptation. A bright white flash (20 J) was used to elicit the mixed rod-cone responses from the dark-adapted eye.

RESULTS

• GENETIC ANALYSES: Five of the six patients with BCD were found to have an identical homozygous IVS6 to 8delTCATACAGGTCATCGCG/insGC mutation in the *CYP4V2* gene (Figures 1 and 2). This mutation was at the 3′ splice site in exon 7 and resulted in the skipping of exon 7, which encodes 62 amino acids. The sixth patient had a novelTrp340X(TGG to TGA; c.954G→A) mutation in the *CYP4V2* gene. The abnormal nucleotide sequence of Trp340X mutation was a transversion of guanine to adenine in the third nucleotide at codon 340 (Figure 2). This alteration caused a substitution of a tryptophan residue resulting in a stop codon at codon 340.

• CLINICAL EXAMINATION: The clinical characteristics of the six unrelated patients are summarized in Tables 1 and 2. Patients' age ranged from 43 to 61 years. The initial symptom was a decrease of visual acuity in two of the patients, night blindness in three, and a constricted visual field in one patient. The visual acuity of the patients ranged from 0.03 to 1.5.

Fundus examination disclosed many small, yellowish-white sparkling spots with a crystalline-like appearance mainly in the posterior poles bilaterally in five cases. These spots were not observed in case 1 because of retinal degeneration and choroidal sclerosis (Figure 3).

Fluorescein angiography revealed a granular hyperfluorescence corresponding to the atrophy of the retinal pigment epithelium with hypofluorescent areas indicating an atrophy or loss of the choriocapillaris. The crystalline deposits did not show hyper- or hypofluorescence (Figure 4).

Goldmann kinetic visual field testing showed a paracentral scotoma and constricted visual field bilaterally in cases 2 and 6. Case 1 had a central scotoma in the right eye and a paracentral scotoma and constricted visual field in the left eye. A mild constriction of the visual filed without a scotoma was observed in case 3. Case 4 had a paracentral